



Sintered Fe-Cu-C Materials

Monnapas Morakotjinda, Rungtip Krataitong, Pongsak Wila, Pisan Siriphol, Anan Daraphan, Ornmanee Coovattanachai, Nattaya Tosangthum, Thanyaporn Yotkaew, Bhanu Vetayanugul and Ruangdaj Tongsri

National Metal and Materials Technology Center (MTEC), 114 Thailand Science Park, Paholyothin Road, Klong Luang, Pathum Thani, 12120 Thailand.

*Author for correspondence; e-mail: sayanm@mtect.or.th

Received: 1 September 2007

Accepted: 1 November 2007.

ABSTRACT

Powder metallurgical method was employed for forming sintered Fe-Cu-C materials from elemental powders. These sintered materials were aimed to be employed as base materials for sintered frictional brake pads. In experimental works, powder mixtures were prepared so that the alloy compositions of Fe-6Cu, Fe-6Cu-1C, Fe-6Cu-2C, Fe-6Cu-3C, Fe-6Cu-4C and Fe-6Cu-5C were obtained. The powder mixtures were processed via a normal 'press and sinter' method. The graphite contents of up to 4 wt. % caused increased strengths and hardness but decreased ductility. Increase of graphite contents of up to 3 wt. % tended to reduce friction coefficient of the sintered materials. In contrast, the sintered Fe-6Cu-5C material exhibited low strengths but high friction coefficient. Microstructural observation and phase identification of the sintered Fe-6Cu-5C material indicated the presence of the mixtures of Ledeburite, cementite and pearlite.

1. BACKGROUND

Powder metallurgy (P/M) is art and science involving with powder production and parts fabrication from metal powders. The P/M has been being increasingly interested by engineering parts manufacturers due to some its benefits. The P/M advantages include high productivity, minimum consumption of raw materials and energy, near net shape character and unique capability of porous material production.

In conventional P/M process [1-6], three basic production steps including compacting, debinding and sintering are very important. The compacting step may be subdivided into three steps, namely powder filling, powder compacting and compact rejecting. Normal concerns for powder filling are powder particle flow, filling height, powder particle

packing and powder particle segregation.

During the compacting step, some phenomena including particle deformation, cold welding at points of contact and interlocking between particles occur. Normal concerns for powder compacting are friction between powder particles and between powder particles/die walls and density distribution of the compact.

During rejecting the compact from the die, spring back, the compact volume expansion to release stored residual stress, is an important factor. The spring back, if occurs too fast with high magnitude, will cause undesirable crack of the compact. Most of the concerns given above have been solved by powder and compacting machine manufacturers. The measurable spring back

has to be known by P/M part designers and manufacturers.

In normal practice, debinding and sintering are carried out in the same furnace. Factors affecting both processes, including temperature, time and atmosphere, have to be optimized. The optimum conditions for debinding and sintering of a certain type powder in the specified furnace are important for obtaining good P/M parts.

Friction materials are used for converting mechanical energy resulting from surface abrasion to heat, which is absorbed and dissipated by the materials. The friction coefficient and shear force between the contacting parts are performance indicators of the friction materials. The friction materials are employed in some applications such as disc brake pad and clutch plate in heavy trucks and off-road vehicles. In these applications the metallic brake lining materials are important components [7]. The metallic brake linings can be based on either copper or iron. Most are produced by using solid state sintering of metallic and inorganic additive powder mixtures. The inorganic additives include ceramic carbides, nitrides and oxides [8].

In this paper, preliminary study on microstructure and property of the sintered Fe-Cu-C materials is presented. The knowledge on the sintered metallic based materials will be a fundamental for further investigation on sintered friction materials.

2. MATERIALS AND METHODS

Powder mixtures were prepared from elemental powders so that the alloy compositions of Fe-6Cu, Fe-6Cu-1C, Fe-6Cu-2C, Fe-6Cu-3C, Fe-6Cu-4C and Fe-6Cu-5C were obtained. The mixed powders were compacted into green tensile test bars with a constant pressure of 600 MPa. The green test bars were then sintered at 1150 °C for 45 minutes in hydrogen. Densities of

green and sintered samples were determined using the Archimedes method. A universal testing machine (Instron model 8801) was employed to measure mechanical properties of the sintered test bars. Hardness of the sintered samples was carried out using a hardness tester (Rockwell scale B). Friction coefficient was measured following the ASTM G133-95 (Linearly reciprocating ball-on-flat sliding wear) with load of 50 N and speed of 600 rpm. Microstructures were also observed using optical microscopy. Phase identification was performed using X-ray diffraction (XRD) technique.

3. RESULTS AND DISCUSSION

3.1 Density

With a constant compacting pressure, green densities of the test bars varied with added graphite contents (Figure 1). When the graphite contents of up to 2 wt. % were added, green densities of the compacts were increased. However, when the graphite contents were higher than 2 wt. % the green densities were decreased. Two factors may govern compactability of the Fe-Cu-C powders. The first is powder particle arrangement. The second is the mass of graphite. With up to 2 wt. %, graphite particles may fill in pores between Fe and Cu powder particles. Pore filling results in increased green density. However, when graphite contents of higher than 2 wt. % were added some graphite particles may substitute the Fe or Cu positions in the compacts. Due to low mass of graphite, the green density is low.

After sintering, densities of the sintered test bars were increased (Figure 1). This indicates that all the test bars were densified after sintering. Variation of sintered density with graphite content was similar to that of green density against carbon content. This suggests that green density, which depends on graphite content, is also the factor controlling final

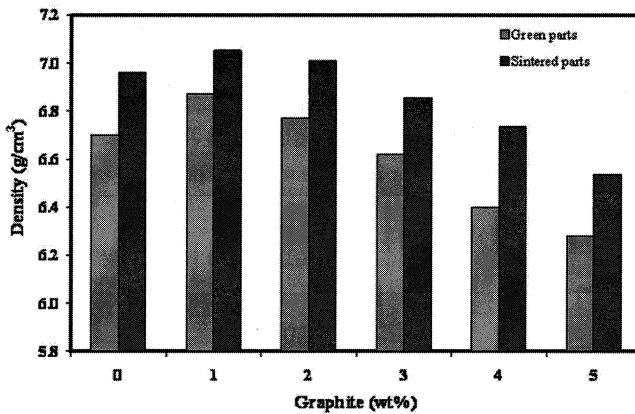


Figure 1. Plot of green and sintered densities of the Fe-Cu-C materials against graphite content.

property of the sintered materials.

3.2 MECHANICAL PROPERTY

Strengths and hardness of the sintered Fe-Cu-C materials (Figure 2) showed similarity with the relationship between sintered density and graphite content. Ductility of the sintered materials obviously decreased with increasing graphite content. With graphite contents of up to 2 wt. %, increases of strengths and

hardness are attributed to strengthening effect of carbon atoms dissolved in Fe-Cu matrix and of precipitation (cementite or Fe_3C) strengthening effect. However, when graphite contents of higher than 2wt. % were added deterioration of strengths and hardness was observed. Decrease of mechanical properties with increasing graphite contents may be attributed to excessive volume fraction of cementite particles.

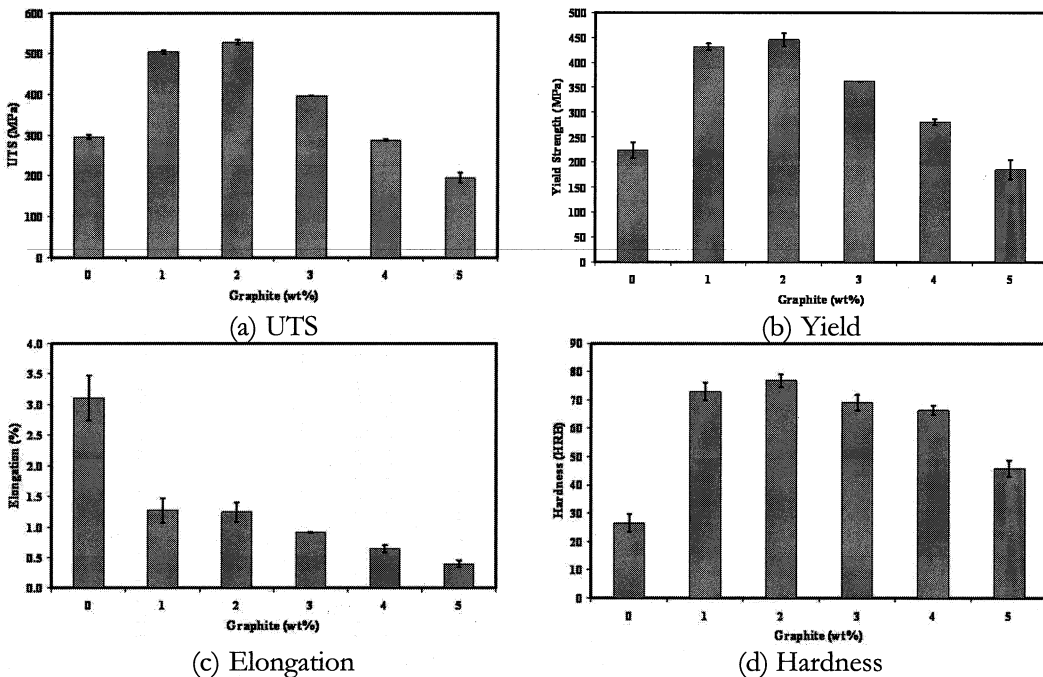


Figure 2. Mechanical properties of the sintered Fe-Cu-C materials.

3.3 Friction and wear property

Experimental results (Figures 3 and 4) showed that under the test conditions, the sintered Fe-6Cu-3C material exhibited the lowest friction coefficient of 0.36 and smallest wear. When graphite contents were increased to 4 and 5 wt. %, the coefficient values were

changed to 0.59 and 0.82 respectively. This may indicate that solid lubricating ability of graphite in the sintered Fe-Cu-C materials is limited at 3 wt. % C. Loss of solid lubricating ability when the graphite content is higher than 3 wt. % is not understood yet.

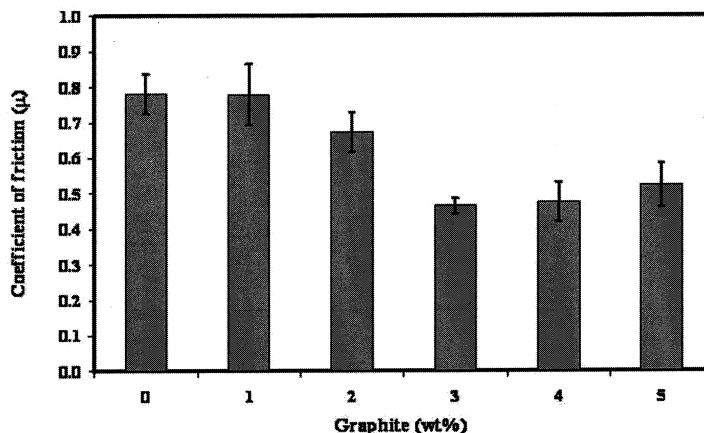


Figure 3. Plot of friction coefficient against graphite content.

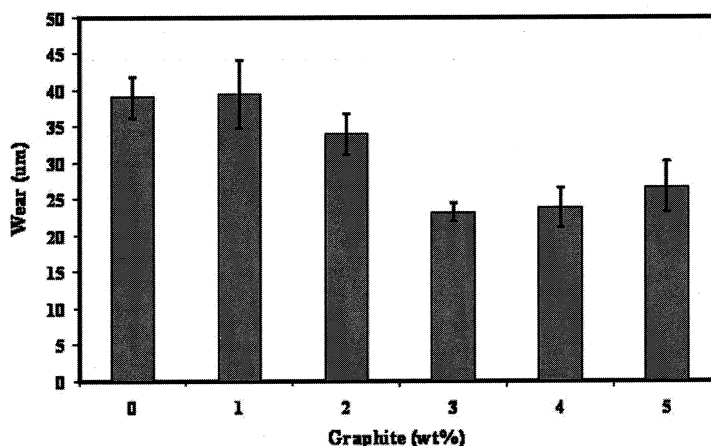


Figure 4. Plot of wear against graphite content.

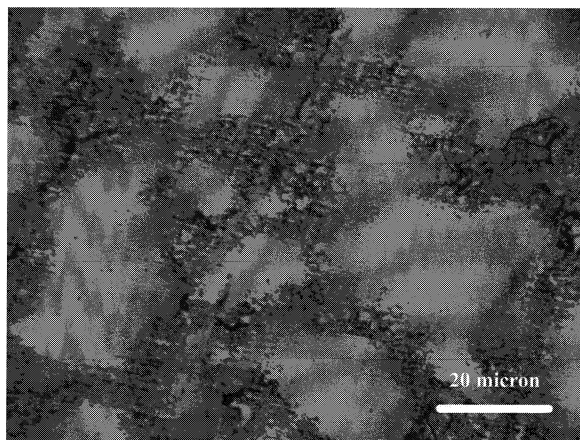
3.4 Microstructure

Microstructure of the sintered materials was dependent on material composition. The sintered Fe-6Cu (Figure 5(a)) exhibited ferritic grains with solid solution (Cu in Fe) gradient. Higher content of Cu was observed along

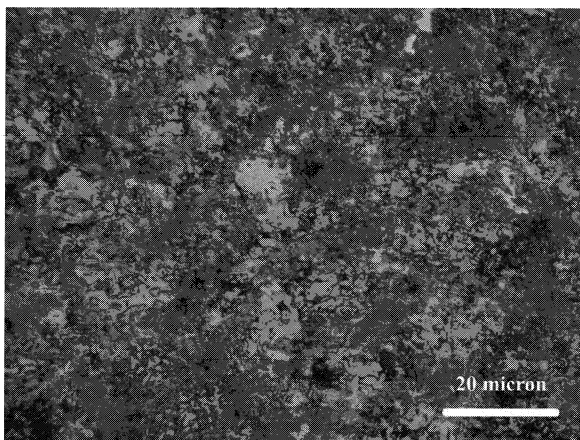
grain boundaries. Microstructure of the sintered Fe-Cu-C materials with carbon contents of less than 1 wt. % consists of ferrite, pearlite, free copper and pores [9, 10]. However, microstructures of the sintered Fe-6Cu-C materials with carbon contents

higher than 1 wt. % exhibited strange feature (Figures 5(b) and (c)). Conventional pearlite feature was hardly observed. Phase

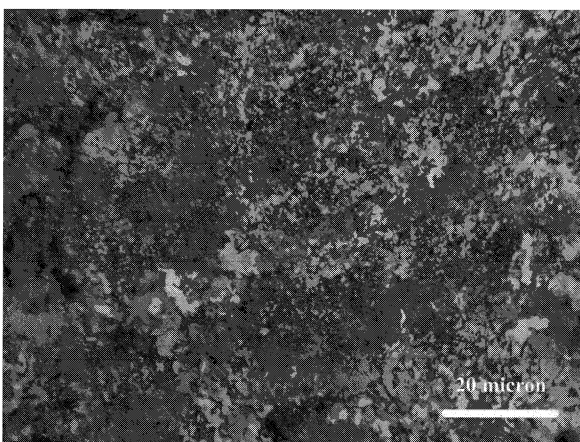
identification by using XRD method was performed to investigate the sintered material microstructures in details (#3.5).



(a) Sintered Fe-6Cu (nital etched)



(b) Sintered Fe-6Cu-2C (picral etched)



(c) Sintered Fe-6Cu-4C (picral etched)

Figure 5. Microstructures of the sintered Fe-Cu-C materials.

3.5 Phase identification by XRD

Phase identification results of the sintered Fe-6Cu-5C material by using XRD are shown in Figure 6 and Table 1. There were 7 diffracted peaks observed. The first diffracted X-ray line was puzzle. The peaks diffracted at $2\theta = 43.259$, 50.500 and 74.000 were identified as diffracted X-ray lines from

austenitic (face-centered cubic) Fe-C phase. The diffracted peaks with $2\theta = 44.580$, 64.801 and 82.200 were the diffracted lines from ferritic (body-centered cubic) Fe-C phase. The XRD results indicated the presence of main ferritic and minor austenitic phases in the sintered high carbon Fe-Cu-C materials.

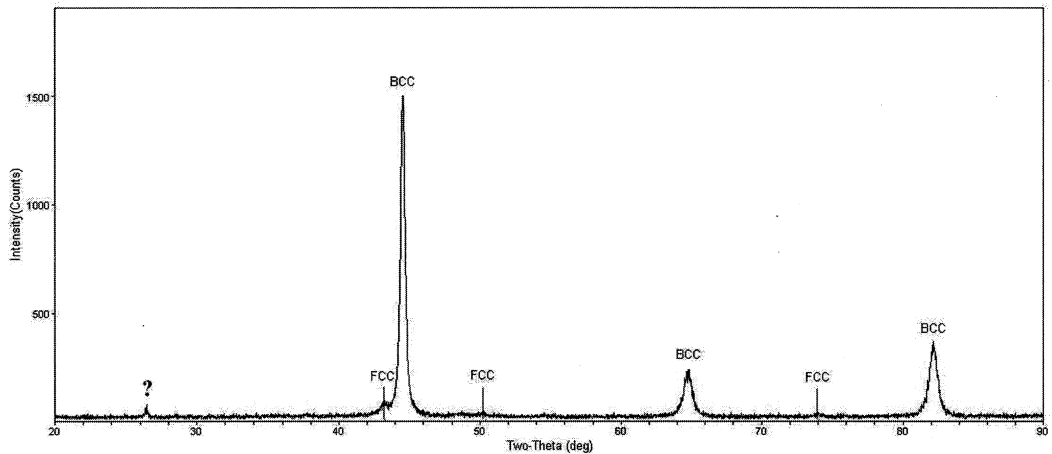


Figure 6. XRD peaks of the sintered Fe6Cu-5C material.

Table 1. Identification of the XRD peaks from the sintered Fe-6Cu-5C material.

2θ	$\sin^2\theta$	$s_1 = (h_1^2 + k_1^2 + l_1^2)$	a_1^*	$s_2 = (h_2^2 + k_2^2 + l_2^2)$	a_2^{**}
43.259	21.630	3	3.619	-	-
44.580	22.290	-	-	2	2.872
50.500	25.250	4	3.612	-	-
64.801	32.400	-	-	4	2.875
74.000	37.000	8	3.620	-	-
82.200	41.100	-	-	8	2.870

* The observed lattice parameter a_1 is corresponding to the lattice parameter of the austenitic Fe phase (face-centered cubic (FCC) phase).

** The observed lattice parameter a_2 is corresponding to the lattice parameter of the ferritic Fe phase (body-centered cubic (BCC) phase).

According to phase diagram of the Fe-C system (Figure 7), the Fe-C materials with carbon contents of higher than 2 wt. % consist of austenite, cementite and ledeburite (eutectics

of austenite and cementite) at high temperatures [11]. The Ledeburite arises when the carbon content is between 2.06% and 6.67%. The eutectic mixture is 4.3% carbon. Its melting

point is 1,147°C. Ledeburite I (close below 1,147 °C) is made of austenite and cementite I. At ambient temperature there exists Ledeburite II. This mixture is composed of cementite I with recrystallized secondary cementite (which separates from austenite as the metal cools) and (with slow cooling) of pearlite. The pearlite results from the eutectoidal decay of the austenite that comes

from the Ledeburite I at 723 °C. During faster cooling, bainite can develop instead of pearlite, and with very fast cooling martensite can develop.

From microstructure, phase identification and phase diagram, it may conclude that the strange features in Figures 5(b) and (c) are mixtures of Ledeburite II, cementite and pearlite.

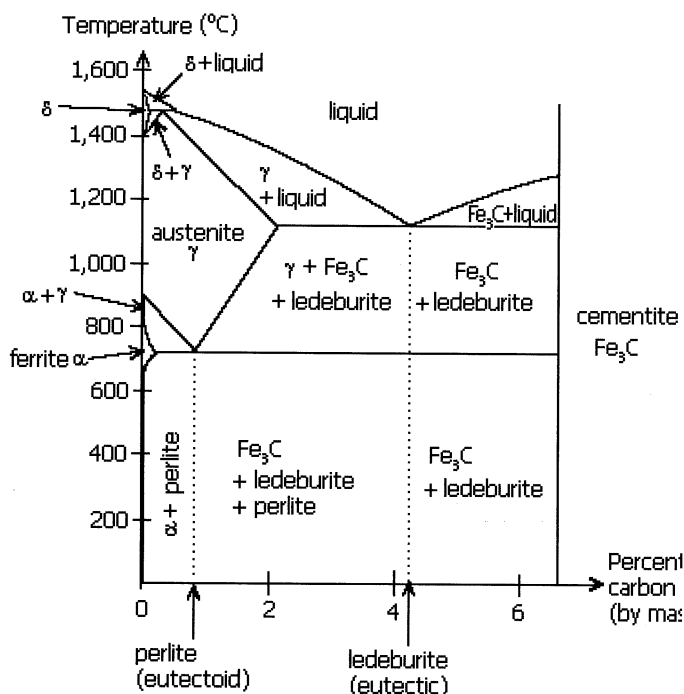


Figure 7. Phase diagram of the Fe-C system [11].

4. CONCLUSIONS

For the sintered Fe-6Cu-C materials, the graphite contents of up to 4 wt. % caused increased strengths and hardness but decreased ductility, compared to the sintered Fe-6Cu material. Increase of graphite contents of up to 3 wt. % tended to reduce friction coefficient of the sintered materials. In contrast, the sintered Fe-6Cu-5C material exhibited low strengths but high friction coefficient. Microstructural observation and

phase identification of the sintered Fe-6Cu-5C material indicated the presence of the mixtures of Ledeburite II, cementite and pearlite.

ACKNOWLEDGEMENTS

The authors would like to express their sincere gratitude to National Metal and Materials Technology Center (MTEC), Pathum Thani, Thailand, for financial support.

REFERENCES

- [1] Thummler F. and Oberacker R. Introduction to Powder Metallurgy, (Jenkins, I and Wood, J. V., Eds.), The Institute of Materials, Cambridge, 1993.
- [2] W. Schatt and K-P. Wieters, Powder Metallurgy: Processing and Materials, European Powder Metallurgy Association, Shrewbury, 1997.
- [3] Jenkins I. and Wood J.V., Powder Metallurgy: An Overview, The Institute of Metals, London, 1991.
- [4] Lenel F.V., Powder Metallurgy: Principles and Applications, Metal Powder Industries Federation, New Jersey, 1980.
- [5] German R.M., Powder Metallurgy and Particulate Materials Processing, Metal Powder Industries Federation, New Jersey, USA., 2005.
- [6] German R.M., Powder Metallurgy of Iron and Steel, John Wiley and Sons, New York, USA., 1998.
- [7] Anderson A.E., Friction and wear of automotive brakes, In: ASM Handbook (Vol.7 Powder metallurgy), ASM International, USA, 1984; 569-577.
- [8] Rohatgi P. K., Liu Y. and Ray S., Friction and wear of metal-matrix composites, In; ASM Handbook (Vol.7 Powder metallurgy), ASM International, USA, 1984; 801-811.
- [9] Beiss P., Dalal K. and Peters R., International atlas of powder metallurgical microstructures, Metal Powder Industries Federation, New Jersey, USA., 2002.
- [10] Huppmann W.J. and Dalal K., Metallographic atlas of powder metallurgy, Verlag Schmid GMBH, Freiburg, 1986.
- [11] Available at http://en.wikipedia.org/wiki/Image:Phase_diag_iron_carbon.PNG